Review of Scientific Instruments

Free space Thomson scattering to study high energy density shocks

Cite as: Rev. Sci. Instrum. **92**, 093503 (2021); https://doi.org/10.1063/5.0048615
Submitted: 24 February 2021 • Accepted: 12 August 2021 • Published Online: 01 September 2021

J. T. Banasek, T. G. Oliver, S. W. Cordaro, et al.

Review of Scientific Instruments ARTICLE scitation.org/journal/rsi

Free space Thomson scattering to study high energy density shocks

Cite as: Rev. Sci. Instrum. 92, 093503 (2021); doi: 10.1063/5.0048615
Submitted: 24 February 2021 • Accepted: 12 August 2021 •
Published Online: 1 September 2021

J. T. Banasek,[a] T. G. Oliver, S. W. Cordaro, and S. C. Bott-Suzuki

AFFILIATIONS

University of California San Diego, La Jolla, California 92093, USA

[a]Author to whom correspondence should be addressed: jbanasek@ucsd.edu

ABSTRACT

A free space collective Thomson scattering system has been developed to study pulsed power produced plasmas. While most Thomson scattering diagnostics on pulsed power machines use a bundle of fibers to couple scattered light from the plasma to the spectrometer, this system used free space coupling of the light, which enabled a spatially continuous image of the plasma. Initial experiments with this diagnostic were performed on an inverse wire array generated by a 200 kA, 1100 ns rise time pulse power generator. The capabilities of this diagnostic were demonstrated by using the low frequency ion acoustic wave feature of the Thomson scattering spectra to measure the plasma flow velocity. The diagnostic was demonstrated to measure velocities between 20 and 40 km/s with an error of 4.7 km/s when fitting with a 600 μm spatial resolution or 8.9 km/s when fitting with a 150 μm spatial resolution. In some experiments, the diagnostic observed a bow shock in the plasma flow as the scattering intensity increased and flow velocity decreased.

I. INTRODUCTION

The study of plasma physics requires accurate and useful diagnostic techniques. One powerful workhorse recently for high energy density (HED) plasmas is collective Thomson scattering, as it can make local measurements of several plasma parameters simultaneously. This regime of Thomson scattering is when the probing wavelength is long enough to see the fluctuations within the plasma, which is defined as when the scattering parameter $\alpha = 1/\lambda_{De}k \gtrsim 1$, where λ_{De} is the electron Debye length and k is defined by $\mathbf{k} = \mathbf{k}_s - \mathbf{k}_l$, where $\mathbf{k}_s$ and $\mathbf{k}_l$ are the scattering and laser wavevectors, respectively. Collective Thomson scattering has been used to study plasmas produced at both laser facilities[1–3] and pulsed power facilities.[4–7] While free space coupling systems have been developed for Thomson scattering at laser-based plasma facilities,[8,9] most pulsed power-based Thomson scattering systems tend to be fiber coupled between the collection from the load and the spectrometer. While this often makes the setup easier and more flexible, its spatial resolution is fundamentally limited to the collection size of a fiber. Though 100 or 200 μm fibers are often used, to reach the desired field of view in these experiments, they were magnified by two to three times resulting in spatial resolutions ranging from 200 to 700 μm. In addition, the fibers can cause challenges in analyzing data if two distinct regions are caught within the same fiber.[10] We therefore developed a free space Thomson scattering system to provide a finer spatial resolution and aid in the studying of shock structures.

This diagnostic was developed for studying the plasma conditions of the radial flow away from a wire in an inverse wire array, which has been useful in understanding traditional wire array experiments.[11] In addition, because of the diagnostically open radial flow, the inverse wire array forms a good platform for shock studies.[12–15] This paper focuses on using the low frequency ion acoustic wave (IAW) feature of the Thomson scattering spectra to measure the radial outflow velocity of plasma from a wire in this experimental configuration.

II. EXPERIMENTAL ARRANGEMENT

The development of this free space Thomson scattering system was performed on the Bertha pulser at University of California San Diego, which provides 200 kA of current with a 1100 ns rise time (Fig. 1). This pulser is a single 3.1 μF capacitor that was charged to 50 kV, discharged using a four-channel trigatron style switch directly into the vacuum load region. The load was a two-wire inverse wire array, as shown in Fig. 2. This setup, with the cathode post in the center connected to the anode through two load wires, allows for an easy diagnosis of the plasma flow conditions, and this plasma flow is useful for shock studies.[12,13] After the plasma forms around the wire, the ablated plasma is driven radially away from the wire, as the

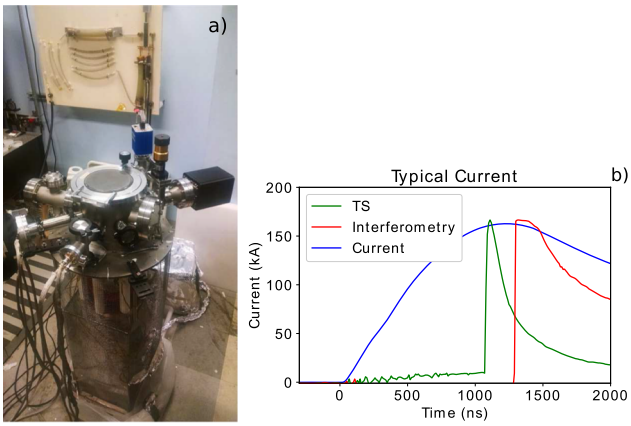

FIG. 1. (a) The Bertha pulser, a 200 kA with a 1110 ns rise time machine. (b) Current (blue) for a typical inverse wire array shot and the diagnostic timings (red and green).

global B field from the current in the central post crossed with the local current density J leads to an outward force. This plasma flow is represented by the gray cones in Fig. 2 and is about 1 mm wide in the diagnostic region.

A free space Thomson scattering system was developed to study this plasma flow. Bertha is a perfect candidate for its design as it is significantly smaller than most other pulsed power machines. This enables a shorter distance to couple the Thomson scattering light from the plasma into the spectrometer, making setting up a free space Thomson scattering system easier than on larger pulsed power facilities.

The free space design used is shown schematically in Fig. 3. The key factors controlling the design were the f-number of the spectrometer, desire to have a large field of view, and the 2 m distance between the load and the slit of the spectrometer. The camera (Andor iStar) has a vertical span of 6.9 mm, which was determined to provide a large enough field of view so that no magnification was needed, and therefore, the f/10 of the spectrometer was the f-number for the entire system. The camera has a resolution of 2048 × 512 with a pixel size of 13.5 μm. For our scattering angle of 135°, this results in a minimum spatial resolution of 19 μm and 9.8 mm field of view along the laser beam.

There are two major challenges with a free space Thomson scattering system; aligning the slit to be parallel to the direction of laser propagation, and reducing off axis losses with the collection up to 3.5 mm off the optical axis. The first challenge is addressed by adding a Dove prism after the collection from the plasma. Rotating a Dove prism along its longitudinal axis rotates the image passing through it, enabling aligning the spectrometer slit to the laser propagation direction.

Off axis losses are a challenge due to a combination of a long travel distance and a large field of view, as off axis points will have a slight angle to the collimated beam and would mostly miss the final focusing optic. By tracing the rays on the extreme edges of the cone from a point in the plasma 3.5 mm off the optical axis to the first lens and through the optical system, the possible losses from these effects are estimated. Using 1 in. optics with focal length of 250 mm and 2 m from the load to the spectrometer slit results in only 17% of the possible light being collected by a 1 in. focusing lens in a two optics system. This is improved by increasing the focusing lens diameter to 2 in. and increasing the light entering the spectrometer to 80%. However, because of this large offset at the focusing lens, only 27% of the light could be collected by the first focusing optic inside the spectrometer. Therefore, a two-lens optical relay was placed between the collection lens and the final focusing lens. This relay was designed to theoretically allow 100% of the light cone collected by the first lens to reach the first focusing lens of the spectrometer.

The laser used in these experiments was a pulsed Nd-YAG laser, which used a single pulse for each experiment. It was used with its frequency doubled to 532 nm wavelength and had an output energy of 1 J and pulse width of 6.5 ns.

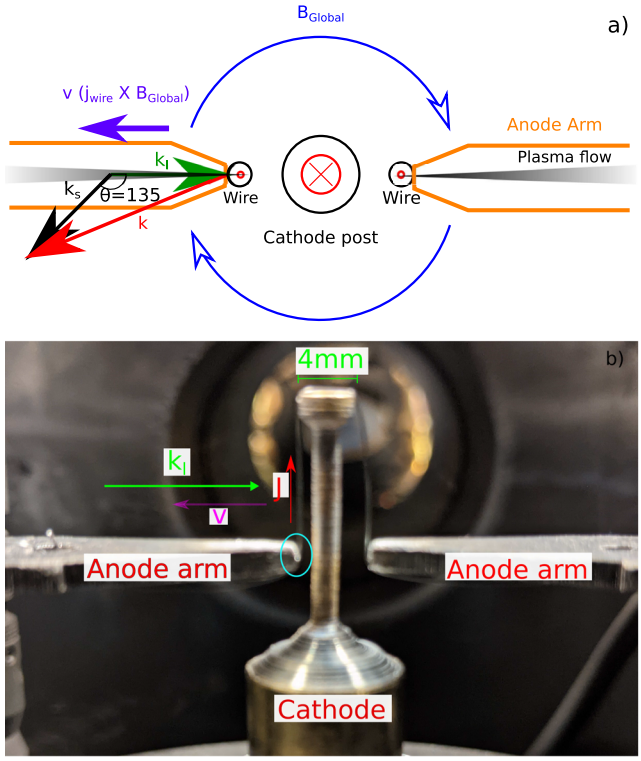

FIG. 2. (a) Top down schematic of the experiment and of the k-vectors relevant to Thomson scattering. (b) Side on picture of the experiment. Cyan circle indicates the interaction region that causes the formation of bow shock.

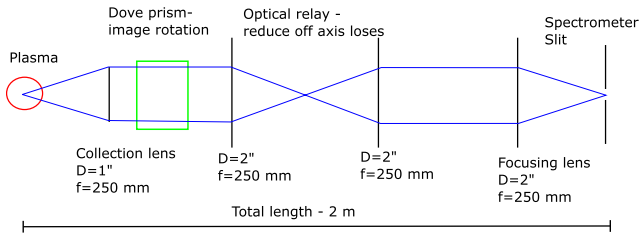

FIG. 3. The schematic setup of the free space Thomson scattering system.

The spectrometer system used was a 750 mm Czerny–Turner spectrometer with a 2400 ℓ/mm grating. The slit width was set to 170 μm, large enough to get most of the scattered light into the spectrometer, resulting in a spectral full width at half-maximum (FWHM) of 0.45 Å. If desired, this spectral resolution could be reduced to 0.3 Å by decreasing the slit width, however, that would decrease the optical throughput of the system. The intensified charge-coupled device (ICCD) camera gate width was 50 ns to ensure that the 6.5 ns laser pulse was captured even if there was jitter between the laser and the camera trigger.

The other diagnostic used in these experiments was a laser interferometer. The interferometer used a frequency doubled Nd-YAG laser with a pulse energy of 150 mJ and a pulse width of 130 ps. The interferometer laser was timed 100 ns after the Thomson scattering pulse and provided an image of the plasma formation during the Thomson scattering measurement.

III. RESULTS

The results presented from this IAW collective Thomson scattering diagnostic will focus on the measurement of the radial outflow velocity of the plasma from a load wire. While it is possible to measure other plasma parameters with IAW Thomson scattering,[16] such as electron temperature, an accurate measurement of those parameters requires a clear spectral resolution of the two IAW peaks. In most cases, we could not clearly resolve both peaks, making accurate measurement of the temperature challenging. Flow velocity measurements, however, do not require resolving the individual peaks, as they are measured as a shift of the entire Thomson scattering profile, and therefore could still be measured. The velocity along the **k** direction, v_k, is measured by a Doppler shift, $\Delta\lambda$, in the IAW profile from the laser wavelength,[16,17]

$$v_k = \frac{c\Delta\lambda}{\lambda_l\sqrt{2(1-\cos(\theta)}}, \tag{1}$$

where θ is the scattering angle. For our scattering angle of 135°, a shift of 1 Å corresponds to a velocity of 30.5 km/s along k. v_k can be converted to v_r using the geometry of the k-vectors relative to the plasma (Fig. 2) and the assumed radial direction of the plasma velocity. This results in $v_r = v_k/\cos(\pi/8)$, or a velocity of 33 km/s for each angstrom of shift from the laser wavelength.

Results of the typical experiment are shown in Fig. 4(a). The raw Thomson scattering signal shows a strong line at the laser wavelength. This line is stray laser light from the Thomson scattering laser hitting the dense plasma around the wire. While this complicates the fitting of the spectrum, it can be corrected by adding a Gaussian profile representing the laser in the synthetic spectrum. To the left of the stray laser line, we see the shifted IAW Thomson scattering spectrum, suggesting an outward radial velocity. We see that the Thomson scattering profile shifts farther away from the laser wavelength as radius increases, showing that the plasma has higher velocity at larger radii. In addition, the Thomson scattering intensity decreases as radius increases, suggesting that the electron density is decreasing with distance from the wire.

Figure 4(b) shows lineouts and fits to the data in Fig. 4(a), where each lineout is a result of summing 32 rows to increase the signal-to-noise ratio (SNR), resulting in a 600 μm spatial resolution. Best fits were performed by minimizing the error between the raw data and

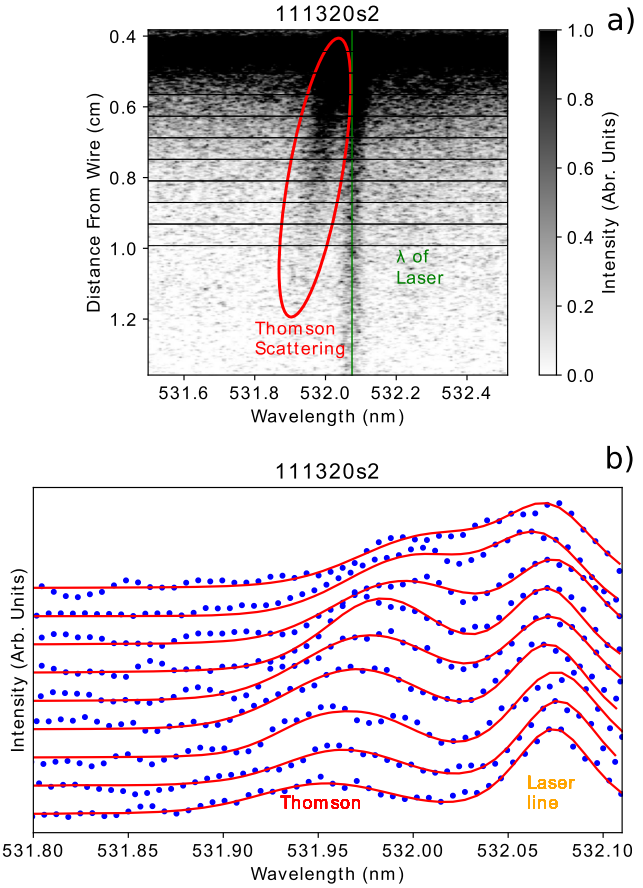

FIG. 4. (a) Raw spectrometer data showing stray light and blue shifted Thomson scattered light. Regions between the white lines are binned for the lineouts in (b). Intensity scale is the number of counts above the no signal background. (b) Fits for the data are shown in part (a) with the best fit to the data (red) and the raw data bin of 32 rows (blue).

a synthetic profile that had flow velocity, electron and ion temperatures, laser wavelength, and relative intensity between the laser and Thomson scattering feature as best fit parameters. While the electron and ion temperatures were used as fitting parameters, as the two peaks could not be discerned, it was challenging to get accurate measurements of these parameters. The closeness of the peaks and the fact that we cannot discern them over the instrumental width suggests that we are working with relatively cold plasmas with a maximum electron temperature of about 10 eV. The fits assumed the electron density was 5×10^{17} cm^{-3}. Though errors in the density do not affect the measured flow velocity, this seems to be a reasonable estimate considering that the plasma is dense enough to be in the region of collective scattering, $\alpha = 1.4$ for these two assumptions, but not dense enough to create significant fringe shifts in the interferometry, where one fringe shift equals an areal density of 4.2×10^{17} cm^{-2}. Having the laser wavelength in the image somewhat complicates fitting, and it does provide an accurate reference of the laser wavelength during the shot. Error bars were estimated assuming that the laser wavelength was accurate within one pixel and the

shift of the Thomson scattering profile was correct within 2 pixels, resulting in an error of 4.7 km/s.

These velocity measurements were used to study the outflow from two different load wire materials, Fe and Mo, which had diameters of 250 and 200 μm, respectively. Figure 5 shows the results from each shot for the different materials. These results were generated by collecting a bin of 32 rows in the spatial direction to increase the SNR. Between 0.5 and 1 cm away from the wire, there is a relatively constant increase in the radial flow velocity of the plasma flow from 20 to 40 km/s. Accurate measurement of the flow velocity at radii smaller than 0.5 cm was challenging due to the fact that the Thomson scattering spectrum was unresolvable from the stray laser light, but it appeared that the velocity is still increasing with increasing radius in that region. We see good agreement in the primary flow velocity between all six shots (three for each material).

These results can also be compared to the previous experimental and simulation work on the wire arrays.[18–20] The earlier work was for a larger current, shorter rise time machine (1.4 MA, 250 ns), and studied wire arrays made of Al or W wires. While our velocity is much lower than found in these earlier experiments (30 vs 100 km/s at 0.7 cm from the wire), we still see that the velocity is increasing for plasma farther away from the wire. This lower velocity could be due to the lower current of the experiment. The insensitivity of the measured flow velocity to the wire material agrees with earlier work that says ablation velocity is approximately consistent over a wide range of array parameters.[18]

While the 32 row bin gives a good general picture of the plasma, the advantage of this free space system is to achieve a higher spatial resolution than with fibers, and therefore, taking lineouts of smaller sizes would be desired. Examples of spectra with 32, 16, and 8 rows summed are shown in Fig. 6(a). These three binning sizes result in spatial resolutions of 600, 300, and 150 μm. Compared to the previous fiber-coupled pulsed power experiments, with a 230 μm spatial resolution, the 8 row bins provide better resolution and a larger field of view (9.8 mm compared to 3.7 mm).[10] To quantify the effect of increased noise on the error bars for the velocity measurements, a Monte Carlo error technique was used.[2,21] Within these Monte Carlo fits, we allowed the linear dispersion of the spectrometer to vary by 1.5%, density by 50%, and ionization state by 10%. These fits result in an average error between 0.6 and 1 cm of 0.79, 1.04, and

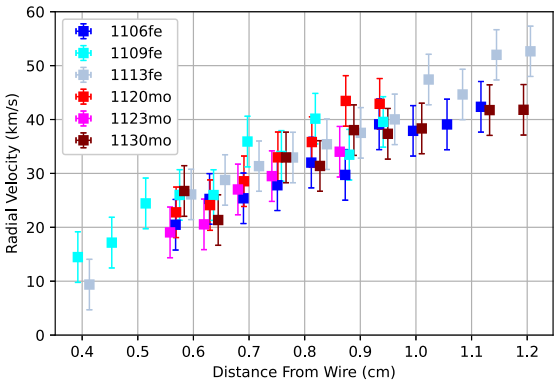

FIG. 5. Measurement of the radial outflow velocity for several Thomson scattering shots with bins of 32 rows to increase the SNR.

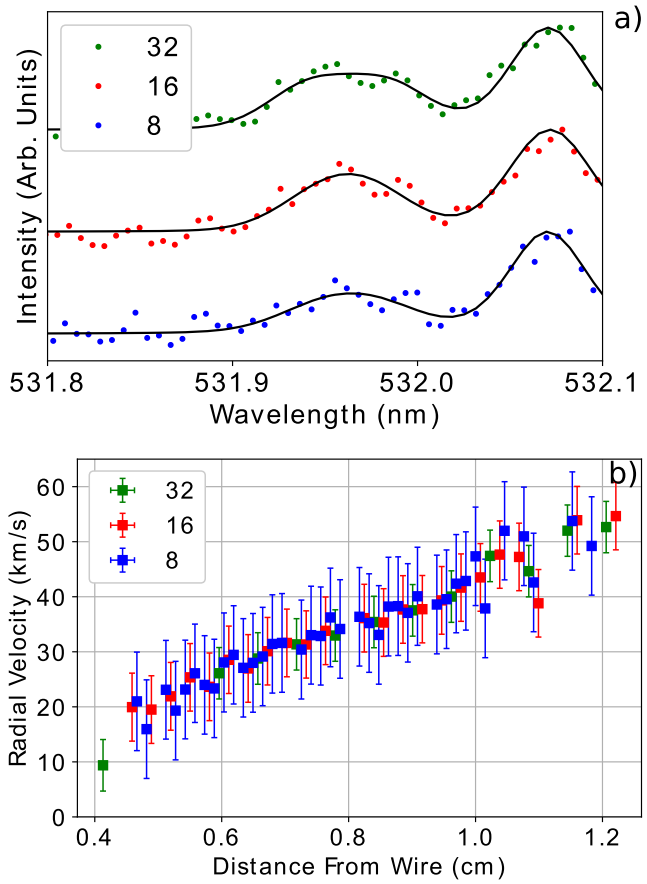

FIG. 6. (a) Comparison of the raw data (circles) and best fits (black) for three different bin sizes (32, 16, and 8 rows) at the same radial location for a single Fe shot. (b) Best fit velocities for a single shot for the three different bin sizes.

1.34 km/s for the 32, 16, and 8 bin sizes, respectively. While this is significantly lower than our estimated error bars of 4.7 km/s, it does show an increase in error for smaller bin numbers. The results in Fig. 6(b) use the differences from the Monte Carlo error calculation as a scaling based on the assumed error for the 32 bin case, resulting in reported errors of 4.7, 6.1, and 8.9 km/s. Even with this increased error, there is a good agreement in the flow velocity for these three different bin sizes [Fig. 6(b)]. However, greater challenges would likely result from this decrease in the SNR when trying to analyze more detailed Thomson scattering features, such as the electron temperature. Therefore, future experiments hope to increase the Thomson scattering signal by using this diagnostic on a larger current pulser that is currently under development at UCSD, which will increase the plasma density, and therefore, the amount of scattering. Plasmas generated from this larger pulser should also be at higher temperatures, enabling the measurement of the electron temperature with this diagnostic.

As the primary purpose of this diagnostic is to aid in the study of shocks, in several of the experiments, we allowed a shock to form in the plasma flow. This shock was created from a slight standoff between the anode arm and the wire, as indicated with the cyan

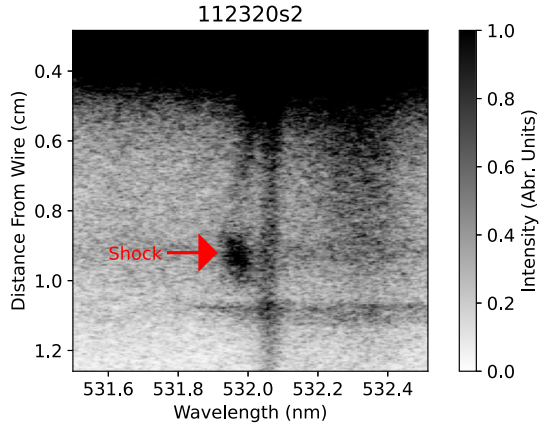

FIG. 7. Results from a Mo shot where there was an obvious shock within the Thomson scattering field of view. The bright region noted is where the plasma slows, indicating a shock.

circle in Fig. 2(b). This standoff causes a bow shock to form the anode arm and continue into the diagnostic region. In these experiments, we noticed that the velocity began to decrease at some radius. The raw data from the spectrometer for one of these types of shots (Fig. 7) show that the continuum and Thomson scattering intensities increase where the velocity changes. Comparing the Thomson scattering velocity data and the interferogram (Fig. 8) shows that a decrease in velocity is at the same point in the interferogram as a tail of a shock formation from the anode arm. This interferogram was taken 100 ns after the Thomson scatting diagnostic and the plasma moved 3 mm in this time; however, the bow shock is formed from the interaction with the anode arm and its position should not move significantly in this time frame. This means that a decrease in velocity and an increase in intensity are due to the flow interacting with this shock. Though not the principal purpose of this study, it does show that this diagnostic should be useful in future shock studies.

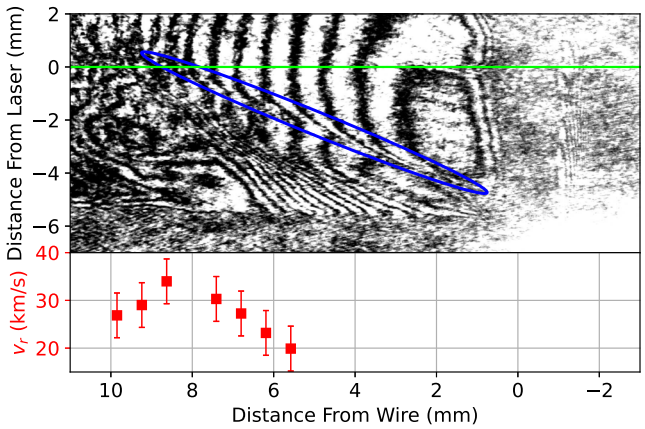

FIG. 8. Interferogram in the top part of figure shows a bow shock coming up from the anode arm (blue oval). The laser is aligned along the green line. The velocity begins to decrease after the bow shock.

IV. CONCLUSION

We have presented results from a new free space Thomson scattering diagnostic, which enables a detailed spatial picture of the changing plasma conditions. Initial capabilities of this diagnostic were demonstrated by measuring the outflow velocity from wires of different materials in an inverse wire array experiment. The diagnostic demonstrated velocity measurements in the range of 20 to 40 km/s, though the measurements of higher velocities could easily be performed. Challenges in measuring plasma temperature resulted due to the plasma conditions of these initial experiments. Future work hopes to use this diagnostic on plasmas with a higher density and temperature to enable the measurement of the electron temperature.

ACKNOWLEDGMENTS

This research was supported by NNSA Stewardship Sciences Academic Programs under DOE Cooperative Agreement No. DE-NA0003764.

DATA AVAILABILITY

The data that support the findings of this study are available from the corresponding author upon reasonable request.

REFERENCES

[1]J. S. Ross, S. H. Glenzer, J. P. Palastro, B. B. Pollock, D. Price, L. Divol, G. R. Tynan, and D. H. Froula, "Observation of relativistic effects in collective Thomson scattering," Phys. Rev. Lett. **104**, 105001 (2010).
[2]R. K. Follett, J. A. Delettrez, D. H. Edgell, R. J. Henchen, J. Katz, J. F. Myatt, and D. H. Froula, "Plasma characterization using ultraviolet Thomson scattering from ion-acoustic and electron plasma waves (invited)," Rev. Sci. Instrum. **87**, 11E401 (2016).
[3]J. S. Ross, P. Datte, L. Divol, J. Galbraith, D. H. Froula, S. H. Glenzer, B. Hatch, J. Katz, J. Kilkenny, O. Landen, A. M. Manuel, W. Molander, D. S. Montgomery, J. D. Moody, G. Swadling, and J. Weaver, "Simulated performance of the optical Thomson scattering diagnostic designed for the National Ignition Facility," Rev. Sci. Instrum. **87**, 11E510 (2016).
[4]G. F. Swadling, S. V. Lebedev, G. N. Hall, S. Patankar, N. H. Stewart, R. A. Smith, A. J. Harvey-Thompson, G. C. Burdiak, P. de Grouchy, J. Skidmore, L. Suttle, F. Suzuki-Vidal, S. N. Bland, K. H. Kwek, L. Pickworth, M. Bennett, J. D. Hare, W. Rozmus, and J. Yuan, "Diagnosing collisions of magnetized, high energy density plasma flows using a combination of collective Thomson scattering, Faraday rotation, and interferometry (invited)," Rev. Sci. Instrum. **85**, 11E502 (2014).
[5]T. Byvank, J. T. Banasek, W. M. Potter, J. B. Greenly, C. E. Seyler, and B. R. Kusse, "Applied axial magnetic field effects on laboratory plasma jets: Density hollowing, field compression, and azimuthal rotation," Phys. Plasmas **24**, 122701 (2017).
[6]J. T. Banasek, S. V. R. Rocco, W. M. Potter, T. Byvank, B. R. Kusse, and D. A. Hammer, "Multi-angle multi-pulse time-resolved Thomson scattering on laboratory plasma jets," Rev. Sci. Instrum. **89**, 10C109 (2018).
[7]J. D. Hare, J. MacDonald, S. N. Bland, J. Dranczewski, J. W. D. Halliday, S. V. Lebedev, L. G. Suttle, E. R. Tubman, and W. Rozmus, "Two-colour interferometry and Thomson scattering measurements of a plasma gun," Plasma Phys. Controlled Fusion **61**, 085012 (2019).
[8]J. Katz, R. Boni, C. Sorce, R. Follett, M. J. Shoup, and D. H. Froula, "A reflective optical transport system for ultraviolet Thomson scattering from electron plasma waves on OMEGA," Rev. Sci. Instrum. **83**, 10E349 (2012).
[9]J. Katz, J. S. Ross, C. Sorce, and D. H. Froula, "A reflective image-rotating periscope for spatially resolved Thomson-scattering experiments on OMEGA," J. Instrum. **8**, C12009 (2013).
[10]J. T. Banasek, S. V. R. Rocco, W. M. Potter, E. S. Lavine, B. R. Kusse, and D. A. Hammer, "Electron plasma wave Thomson scattering on laboratory plasma jets," Phys. Plasmas **27**, 062708 (2020).

[11]A. J. Harvey-Thompson, S. V. Lebedev, S. N. Bland, J. P. Chittenden, G. N. Hall, A. Marocchino, F. Suzuki-Vidal, S. C. Bott, J. B. A. Palmer, and C. Ning, "Quantitative analysis of plasma ablation using inverse wire array Z pinches," Phys. Plasmas **16**, 022701 (2009).
[12]J. L. Peebles, S. C. Bott, K. Gunasekera, J. Kim, L. Harpster, B. Evans, D. Gomez, O. Paran, C. Peterson, and F. N. Beg, "Examination of bow-shock formation in supersonic radiatively cooled plasma flows," IEEE Trans. Plasma Sci. **39**, 2422–2423 (2011).
[13]S. C. Bott-Suzuki, L. S. Caballero Bendixsen, S. W. Cordaro, I. C. Blesener, C. L. Hoyt, A. D. Cahill, B. R. Kusse, D. A. Hammer, P. A. Gourdain, C. E. Seyler, J. B. Greenly, J. P. Chittenden, N. Niasse, S. V. Lebedev, and D. J. Ampleford, "Investigation of radiative bow-shocks in magnetically accelerated plasma flows," Phys. Plasmas **22**, 052710 (2015).
[14]L. G. Suttle, G. C. Burdiak, C. L. Cheung, T. Clayson, J. W. D. Halliday, J. D. Hare, S. Rusli, D. R. Russell, E. R. Tubman, A. Ciardi, N. F. Loureiro, J. Li, A. Frank, and S. V. Lebedev, "Interactions of magnetized plasma flows in pulsed-power driven experiments," Plasma Phys. Controlled Fusion **62**, 014020 (2020).
[15]S. V. Lebedev, L. Suttle, G. F. Swadling, M. Bennett, S. N. Bland, G. C. Burdiak, D. Burgess, J. P. Chittenden, A. Ciardi, A. Clemens, P. De Grouchy, G. N. Hall, J. D. Hare, N. Kalmoni, N. Niasse, S. Patankar, L. Sheng, R. A. Smith, F. Suzuki-Vidal, J. Yuan, A. Frank, E. G. Blackman, and R. P. Drake, "The formation of reverse shocks in magnetized high energy density supersonic plasma flows," Phys. Plasmas **21**, 056305 (2014).
[16]D. Froula, S. H. Glenzer, N. C. J. Luhmann, and J. Sheffield, *Plasma Scattering of Electromagnetic Radiation: Theory and Measurement Techniques*, 2nd ed. (Elsevier, Amsterdam, 2011), p. 520.
[17]S. V. R. Rocco, J. T. Banasek, W. M. Potter, and D. A. Hammer, "Time-resolved Thomson scattering on gas-puff Z-pinch plasmas at pinch time," IEEE Trans. Plasma Sci. **89**, 10C117 (2018).
[18]J. P. Chittenden, S. V. Lebedev, B. V. Oliver, E. P. Yu, and M. E. Cuneo, "Equilibrium flow structures and scaling of implosion trajectories in wire array Z pinches," Phys. Plasmas **11**, 1118–1127 (2004).
[19]A. J. Harvey-Thompson, S. V. Lebedev, S. Patankar, S. N. Bland, G. Burdiak, J. P. Chittenden, A. Colaitis, P. De Grouchy, G. N. Hall, E. Khoory, M. Hohenberger, L. Pickworth, F. Suzuki-Vidal, R. A. Smith, J. Skidmore, L. Suttle, and G. F. Swadling, "Optical Thomson scattering measurements of cylindrical wire array parameters," Phys. Plasmas **19**, 056303 (2012).
[20]A. J. Harvey-Thompson, S. V. Lebedev, S. Patankar, S. N. Bland, G. Burdiak, J. P. Chittenden, A. Colaitis, P. De Grouchy, H. W. Doyle, G. N. Hall, E. Khoory, M. Hohenberger, L. Pickworth, F. Suzuki-Vidal, R. A. Smith, J. Skidmore, L. Suttle, and G. F. Swadling, "Optical Thomson scattering measurements of plasma parameters in the ablation stage of wire array *Z* pinches," Phys. Rev. Lett. **108**, 145002 (2012).
[21]J. T. Banasek, T. Byvank, S. V. R. Rocco, W. M. Potter, B. R. Kusse, and D. A. Hammer, "Time-resolved Thomson scattering on laboratory plasma jets," IEEE Trans. Plasma Sci. **46**, 3901–3905 (2018).